# Fractional-Delay Sequential Blind Beamforming for Wireless Multipath Communications in Confined Areas

Salma A. Farès, Tayeb A. Denidni, *Senior Member, IEEE,* Sofiène Affès, *Senior Member, IEEE,* and Charles Despins, *Senior Member, IEEE*

***Abstract*— This paper presents a new adaptive antenna-array beamforming receiver for multipath correlated signals in hostile environments, such as indoor confined or underground areas, where intersymbol interference (ISI) and intrasymbol interference (isi) are predominant. The proposed receiver uses a new synchronization approach for multipath propagation and is based on sequential blind CMA and nested LMS beamformings with adaptive fractional-time-delay estimation. This approach uses on one hand CMA and LMS to recover any time path arrival (TPA) that is an integer multiple of the sampling interval, and nested adaptive fractional time delay estimation with LMS on the other hand to recover any TPA that is a non-integer multiple of the sampling interval. Coherent Maximum Ratio Combining (MRC) with hard Decision Feedback Identification (DFI) is also proposed for optimal and constructive combination of these different extracted paths. Analysis and results show the promising performance of the new adaptive antenna-array structure for different operating conditions and modulation schemes.**

***Index Terms*— Adaptive arrays, constant modulus algorithm (CMA), Least mean square methods, fractional delay filter, intersymbol interference, diversity system.**

## I. Introduction

THE main cause of degradation of communication quality in harsh confined environments, such as underground mines, is multipath fading as it is typically more severe than co-channel interference (CCI) [1, 2]. Usually underground communication systems are based on IEEE 802.11 standard using carrier sense multiple access with collision avoidance (CSMA-CA) that minimizes the CCI problem and leaves multipath fading as the main source of errors. This multipath phenomenon arises when a transmitted signal undergoes reflection from various obstacles in the propagation environment. This gives rise to multiple waves arriving at the receiver from different directions with different amplitudes, phases and time delays, which inflicts intersymbol interference (ISI) and intrasymbol interference (isi) on the received signal and consequently time dispersion and fading [3, 4]. To provide a remedy, adaptive equalizers [4], error-correcting codes [5], diversity [6], RAKE receivers for code division multiple access (CDMA) [7, 18, 26], Coded Orthogonal Frequency Division Multiplexing [8], and adaptive antenna arrays (AAA) [9-11] have been proposed. Among these, AAA techniques exploit spatial diversity by using multiple antennas. They have the potential of achieving high data rates and increasing the capacity of mobile services by effectively reducing the multipath effect and CCI.

Adaptive antenna beamforming has been shown to be an effective mean for combating CCI and multipath propagation. Recently many different types of antenna beamforming have been developed [12, 13], and their design employs some information about the desired signal such as using a training sequence. Their use not only reduces the capacity of the system but also requires synchronization between the incident desired signal and the reference (sequence) one. Therefore, there is a strong demand for blind algorithms. For instance, the constant modulus algorithm (CMA) [14], applied in a blind AAA, is considered as a promising method in mobile communications for mitigating multipath fading and suppressing CCI signals. Unlike the least-mean-square (LMS) algorithm [15], CMA-AAA does not need synchronization between the incident desired signal and the reference signal. It improves the received signal by suppressing not only the CCI signals, but also the delayed paths of the desired signal [14]. However, suppressing the multipath rays of the desired signal wastes a part of the available power and requires additional degrees of freedom, i.e., more array elements. In addition, since these arriving paths are delayed replicas of an identical source, it is desirable to separate and combine the delayed paths instead of suppressing them for received power maximization.

Several methods have been proposed to separate and combine the delayed paths. Among them, we mention the spatial-domain path-diversity methods [16- 17] for time division multiple access systems, based on spatial processing for efficient exploitation of the propagated energy. In these methods, multiple beams are formed to separate the direct path and the delayed paths by using training sequences. Paths with various time delay differences are separately extracted at the receiver to produce each of the multiple paths in the spatial domain. Then, the time delay difference is corrected, and the waves are combined.

These aforementioned approaches have certain advantages and limitations, some of them require training sequences and all of them aim to solve the problem of ISI in multipath

Manuscript received August 17, 2006; accepted February 1, 2007. The associate editor coordinating the review of this manuscript and approving it for publication was M. Shafi. This work was supported by NSERC and Bell Nordic Group, Inc.

The authors are with INRS-ÉMT, Montréal, QC, Canada and Underground Communications Research Laboratory, Val-d'or, QC, Canada (e-mail: {aitfares, denidni, affes}@emt.inrs.ca). C. Despins is also with Prompt-Quebec, Montréal, QC, Canada, (e-mail: cdespins@promptquebec.com).

Digital Object Identifier 10.1109/TWC.2008.060596.

propagation environments, when the time path arrival (TPA) is an integer multiple of the sampling interval. Regarding the isi problem, when the TPA is non-integer multiple of the sampling interval, other approaches are used such as Rake receiver, applied in CDMA systems, to treat the path arrivals at the chip interval [7, 18, 26] or straightforwardly, over-sampling [4, 19] is employed. However, over-sampling will complicate the structure of the analog-to-digital converter, and also may not synchronize correctly within the actual time path arrival $\tau$.

Generally speaking, when the TPA is a non-integer multiple of the sampling interval, the power available in these paths is wasted and the fractional time delay estimation (FTDE) is called for to overrule the over-sampling solution. FTDE filters are employed in several signal processing applications such as the estimation of the time delay difference between signals received at two spatially separated array antennas [20]. They consist in using a first-order or linear interpolator to implement a Fractional Delay Filter (FDF) [20]. An FDF is a type of digital filter designed for band-limited interpolation, which can be implemented using a Finite Impulse Response (FIR) filter based on the truncated $sinc$-interpolation method [21].

In this paper, we present a new approach using sequential blind spatial-domain path-diversity beamforming (SBB) to remedy both the ISI and isi problems using jointly CMA, LMS and adaptive FTDE filtering. This approach is designed to sequentially recover multipath rays by using multiple beamformings for received power maximization. First, the strongest path is extracted using the Modified-CMA (MCMA) [22-24]. Second, the paths coming with delays that are multiple integers of the sampling interval are estimated using Integer Delay-CMA (ID-CMA) filters adapted using LMS with the CMA delayed output as a reference signal [23]. Finally, the paths coming with fractional delays are estimated using Fractional Delay-CMA (FD-CMA) filters [24] adapted using LMS and FTDE, the latter is implemented by an FIR $sinc$-interpolation filter [20]. Furthermore, by relying on the common phase ambiguity characteristic presented in these extracted paths, additional enhancement is obtained by using a modified coherent Maximum Ratio Combining (MRC) detector with hard Decision Feedback Identification (DFI) [18, 25, 26] to constructively combine the different received paths for signal-to-noise ratio (SNR) maximization.

The paper is organized as follows. Section 2 presents the signal model. The proposed SBB algorithm and its mathematical formulations are described in Section 3. The performance of the SBB by computer simulation results is presented in Section 4. Concluding remarks are given in Section 5.

## II. Signal Model

Consider a uniform linear array[1] of $N$ omni-directional-antenna elements receiving $L$ multipath signals. The received signal $x_m(k)$ at the $m$-th antenna can be expressed as:

$$x_m(k) = \sum_{i=1}^{L} \alpha_i(k) s(k-\tau_i) e^{-j\pi(m-1)sin(DoA_i)} e^{-2\pi f_D k} + \eta_m(k), \tag{1}$$

where, $\alpha_i(k)$ are the complex gains of the Rayleigh fading rays (with uniformly distributed phases $\varphi_i$ between 0 and $2\pi$) of the $i$-th path; $\alpha_i(k)e^{-2\pi f_D k}$ are of Jakes' model with $f_D$ as maximum Doppler spread[2], $s(k)$ is the desired source sequence, drawn from alphabet members $A_M = \{a_1, \ldots, a_M\}$, $L$ is the number of multipath signals, $\tau_i$ is the path delay for the $i$-th path, $DoA_i$ is the direction of arrival of the $i$-th path and $\eta_m(k)$ are additive white Gaussian noise processes with variance $\sigma_n^2$ at the $m$-th receive antenna. For convenience, the array is assumed to be uniform and linear with inter-element spacing $d = \lambda/2$, where $\lambda$ is the wavelength at the operating frequency.

The received signal vector representation is given by:

$$\mathbf{x}(k) = \mathbf{A}_s(k) \cdot \mathbf{s}(k) + \underline{\eta}(k), \tag{2}$$

where $\mathbf{A}_s$ is an $N \times L$ matrix whose columns $\mathbf{a}_s(\theta_k)$ for $k = 1, \ldots, L$ are determined by the propagation vector and $\mathbf{s}(k) = [\alpha_1 s(k-\tau_1) \ldots \alpha_L s(k-\tau_L)]^T$. For simplicity, the first path is assumed the strongest one.

## III. Proposed Sequential Blind Beamforming (SBB) Method

### A. Background

According to statistical modeling in [27] of the studied underground channel, we were able to characterize, among many other channel parameters, the maximum number of paths at a given operation frequency and a given path resolution. Thus, we can assume for a given transmission rate and modulation type that the maximum number of paths arriving with delays that are a multiple integer of the sampling interval as well as the maximum number of paths arriving with fractional-time delays are both predicted accurately. Consequently, we assume $n$ paths causing ISI and $p$ paths causing isi. To simplify, the following study is performed using a three-path channel model for illustration purposes where the TPAs are given by $\tau_1 = 0$ (the strongest path), $\tau_2 = \tau < T_s$, and $\tau_3 = T_s$.

Figure 1 shows the new structure for spatial-domain path-diversity to resolve multipath signals when TPAs are both integer (0, $T_s$) and non-integer ($\tau$) multiples of the sampling interval. This method is implemented using three sequential beamformers. The first beamformer is used to estimate the strongest path, and its weights ($\mathbf{w}_{MCMA}(k)$) are adapted using the MCMA. The output of this filter ($y_{MCMA}(k)$) is fed into both the ID-CMA and FD-CMA beamformers to construct the path arriving with an integer delay $\tau_3 = T_s$ and the path arriving with a fractional delay $\tau_2 = \tau$, respectively, using the LMS algorithm. However, to ensure that the FD-CMA

[1]The proposed algorithm does not have any constraint on the choice of such antenna array configuration. For the sake of simplicity, we used this configuration.

[2]We chose here the model of a point-source propagation with no angular distribution to consider the worst-case scenario in terms of performance. However, the proposed algorithm can be applied to any channel type or angular distribution without limitation in principle.

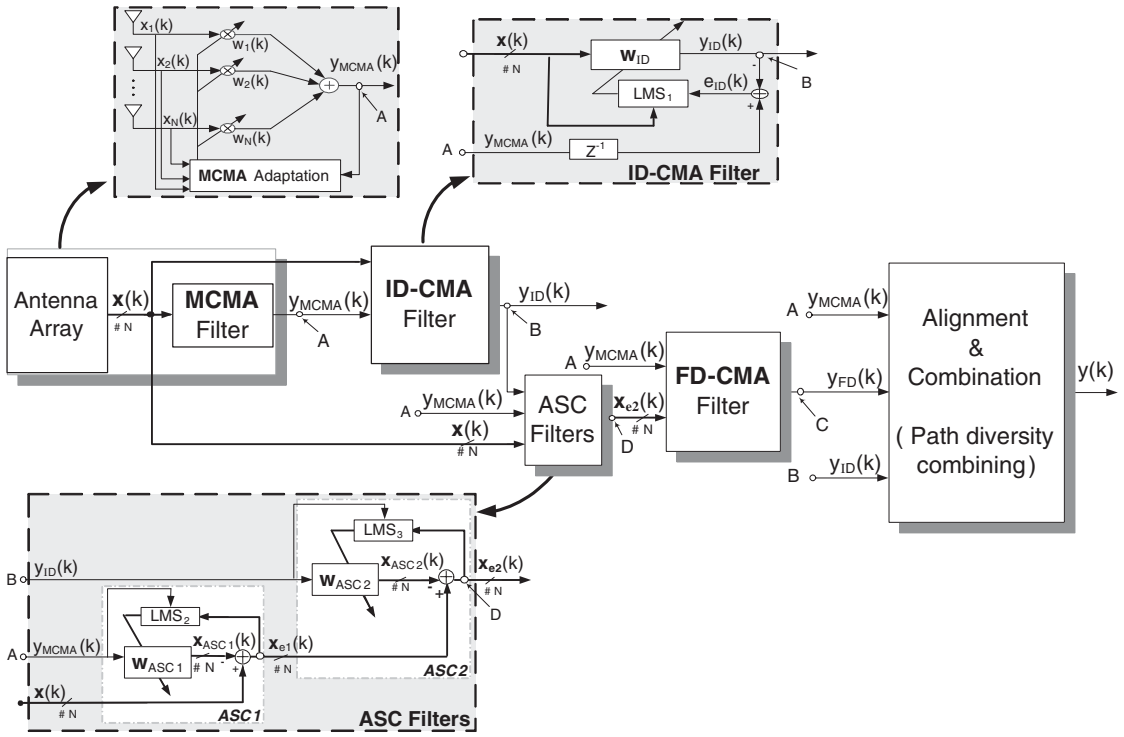


Fig. 1. Proposed Sequential Blind Beamforming (SBB) algorithm.

filter detect the path arriving with a fractional delay and not the others, adaptive signal cancellers (ASC) [28] are used to extract the other contributions from the received signal vector. Finally, MRC with hard DFI is used to combine these extracted paths. Detailed explanations of the entire blocks are given in the following sections.

### *B. Modified -CMA Adaptive Antenna Array*

The block diagram of an adaptive antenna array is shown in Fig.1, where the signals received by a multiple-antenna array are weighted and combined to generate the output signal. Given a beamformer weight vector $\mathbf{w}_{CMA}(k)$, the output of the CMA-beamformer is given by:

$$y_{CMA}(k) = \mathbf{w}_{CMA}^{H}(k) \cdot \mathbf{x}(k). \tag{3}$$

The CMA-AAA aims to eliminate the amplitude fluctuation of the array output signal due to interferences. Therefore, the cost function to be minimized is represented as:

$$J(\mathbf{w}_{CMA}) = E[(|y_{CMA}(k)|^2 - R_{CMA})^2], \tag{4}$$

where $E[.]$ denotes the ensemble mean, and $R_{CMA}$ is a constant, which depends on the input symbols $a$. This constant is defined by:

$$R_{CMA} = \frac{E[|a|^4]}{E[|a|^2]}, \tag{5}$$

for $a \in A_M$.

Since CMA is phase blind, the array output has an arbitrary phase rotation at convergence. To address this problem, a MCMA algorithm is used next where the cost function now is divided into real and imaginary parts as follows:

$$\begin{aligned} J(\mathbf{w}_{MCMA}) =& E[(|y_{MCMA_R}(k)|^2 - R_R)^2] \\ &+ E[(|y_{MCMA_I}(k)|^2 - R_I)^2], \end{aligned} \tag{6}$$

where $R_R$ and $R_I$ are real constants defined by:

$$R_R = \frac{E[|a_R(n)|^4]}{E[|a_R(n)|^2]}, \tag{7}$$

$$R_I = \frac{E[|a_I(n)|^4]}{E[|a_I(n)|^2]}, \tag{8}$$

$$a_R(n) = real(a(n)), \tag{9}$$

$$a_I(n) = imag(a(n)), \tag{10}$$

and

$$y_{MCMA_R}(k) = real(y_{MCMA}), \tag{11}$$

$$y_{MCMA_I}(k) = imag(y_{MCMA}). \tag{12}$$

A stochastic gradient search method is used to minimize the MCMA cost function by adaptively adjusting the weight vector $\mathbf{w}_{MCMA}$ according to:

$$\mathbf{w}_{MCMA}(k+1) = \mathbf{w}_{MCMA}(k) - \mu \cdot e^*(k) \cdot \mathbf{x}(k), \tag{13}$$

where $\mu$ is a small positive step size and the error function is given by:

$$e(k) = e_R(k) + j e_I(k), \tag{14}$$

where,

$$e_R(k) = y_{MCMA_R} \cdot (y^2_{MCMA_R}(k) - R_R), \tag{15}$$

$$e_I(k) = y_{MCMA_I} \cdot (y^2_{MCMA_I}(k) - R_I). \tag{16}$$

In this case the output of this Modified-CMA filter is given by:

$$y_{MCMA}(k) = \mathbf{w}_{MCMA}^{H}(k) \cdot \mathbf{x}(k). \tag{17}$$

### C. ID-CMA Filter

The integer delay path is extracted sequentially by using a delayed replica ($y_{MCMA}(k-1)$) from the estimated signal ($y_{MCMA}(k)$) as a reference signal for the LMS algorithm to construct the $2^{nd}$ beamformer [23] as illustrated in the blowup of the block ID-CMA filter shown in Fig. 1. Given a beamformer weight vector $w_{ID}(k)$, the output of the ID-CMA filter is obtained as:

$$y_{ID}(k) = \mathbf{w}_{ID}^{H}(k) \cdot \mathbf{x}(k). \quad (18)$$

This weight vector $w_{ID}(k)$ is adjusted using LMS as follows:

$$\mathbf{w}_{ID}(k+1) = \mathbf{w}_{ID}(k) + \mu_1 . e_{ID}^{*}(k) . \mathbf{x}(k), \quad (19)$$

where $\mu_1$ is a positive step size and the error signal is calculated using the delayed replica of $y_{MCMA}(k)$ (i.e. ($y_{MCMA}(k-1)$) as a reference signal, and it is given by:

$$e_{ID}(k) = y_{MCMA}(k-1) - y_{ID}(k). \quad (20)$$

After estimating the paths coming with integer multiples of the sampling interval ($\tau_1$ and $\tau_3$), the fractional path delay estimation procedure will be explained below.

### D. Adaptive Signal Canceller (ASC)

To ensure that the FD-CMA filter detect the fractional path delay and not the others, the latter contributions are removed from the received signal vector $\mathbf{x}(k)$. To perform this extraction, two adaptive signal cancellers (ASC1 and ASC2) are used successively, as depicted in the blowup of the block ASC filters shown in Fig.1. The output vectors of the ASC1 and ASC2 filters are given as:

$$\mathbf{x}_{ASC1}(k) = \mathbf{w}_{ASC1}^{H}(k) . y_{MCMA}(k)), \quad (21)$$

$$\mathbf{x}_{ASC2}(k) = \mathbf{w}_{ASC2}^{H}(k) . y_{ID}(k). \quad (22)$$

By using the received signal vector $\mathbf{x}(k)$ and the ASC1 error signal vector $\mathbf{x}_{e1}(k)$ as reference signals for the ASC1 and ASC2 filters, respectively, the error signal vectors for ASC1 and ASC2 can be written as:

$$\mathbf{x}_{e1}(k) = \mathbf{x}(k) - \mathbf{x}_{ASC1}(k), \quad (23)$$

$$\mathbf{x}_{e2}(k) = \mathbf{x}_{e1}(k) - \mathbf{x}_{ASC2}(k). \quad (24)$$

Therefore, the weight vectors for the ASC1 and ASC2 filters are adapted with the LMS algorithm as follows:

$$\mathbf{w}_{ASC1}(k+1) = \mathbf{w}_{ASC1}(k) + \mu_2 \cdot \mathbf{x}_{e1}^{H}(k) . y_{MCMA}(k), \quad (25)$$

$$\mathbf{w}_{ASC2}(k+1) = \mathbf{w}_{ASC2}(k) + \mu_3 \cdot \mathbf{x}_{e2}^{H}(k) . y_{ID}(k), \quad (26)$$

where $\mu_2$ and $\mu_3$ are positive step sizes.

### E. FD-CMA Filter

After this extraction, the received signals collected at points A and D, as shown in Fig. 1, can be expressed, respectively, by:

Point A

$$y_{MCMA}(k)) = \hat{s}(k) + \gamma_1(k), \quad (27)$$

Point D

$$\mathbf{x}_{e2}(k) = \underline{\beta}(k) s(k-\tau) + \underline{\gamma}_2(k), \quad (28)$$

where, $\hat{s}(k)$ is an estimation of the transmitted symbol $s(k)$, $\underline{\beta}(k)$ is a multiplicative factor vector that represents the impulse response vector of the path arriving with the fractional delay $\tau$ at the antenna array, and $\gamma_1(k)$ and $\underline{\gamma}_2(k)$ are additive white Gaussian noises.

By summing the vector $\mathbf{x}_{e2}(k)$ at point D, the points A and E shown in Fig.2a can be regarded as two spatially separated antenna elements. The received signal collected at point E can be expressed by:

$$y_{e2}(k) \simeq \beta(k) . s(k-\tau) + \gamma(k), \quad (29)$$

where, $\beta(k) = \sum_{i=1}^{N} \underline{\beta}_i(k)$, $\gamma(k) = \sum_{i=1}^{N} \underline{\gamma}_{2,i}(k)$ and $y_{e2}(k) = \sum_{i=1}^{N} \mathbf{x}_{e2,i}(k)$.

Consequently, by analogy with the FDF proposed in [20], the fractional delay between the signals $s(k)$ and $s(k-\tau)$ can be estimated as shown in Fig.2a. This FTDE filter consists of a linear interpolator which can be implemented using an FIR filter based on the truncated $sinc$-interpolation method.

However, instead of summing directly the signal $\mathbf{x}_{e2}(k)$ at point D (as shown in Fig.2a) to construct the reference signal of the FTDE filter, the filter $\mathbf{w}_{FD}(k)$ is inserted to construct the FD-CMA filter and estimate the fractional delay path as depicted in Fig.2b. The weight vector of this filter ($\mathbf{w}_{FD}(k)$) is adapted using LMS algorithm ($\text{LMS}_5$ in Fig.2b), where the first beamformer output $y_{MCMA}(k)$ is fed into the FTDE filter to generate a reference signal. The weight adaptation for both FTDE and $\mathbf{w}_{FD}$ filters is nested in the sense that the output of the $\mathbf{w}_{FD}$ filter is used as a reference signal for FTDE filter and vice-versa.

#### 1) Fractional Time Delay Estimation:

Once the first path is estimated by MCMA filter, it is delayed by an estimated value $\hat{\tau}$ using the fractional delay filter $\boldsymbol{H}$. This filtering is carried out by using the following equation detailed in the Appendix:

$$\begin{aligned} y_h(k) &\cong y_{MCMA}(k-\hat{\tau}) \\ &= \sum_{i=-\infty}^{+\infty} sinc(n-\hat{\tau}) . y_{MCMA}(k-n) \\ &= \sum_{i=-P}^{+P} sinc(n-\hat{\tau}) . y_{MCMA}(k-n), \end{aligned} \quad (30)$$

where the infinity sign in the summation is replaced by an integer $P$, which is chosen sufficiently large to minimize the truncation error. $\hat{\tau}$ is the instantaneous estimated time delay. This delayed signal $y_h(k)$ is the output of the FIR filter $\boldsymbol{H}$ whose coefficients are $sinc(n-\hat{\tau})$ and input is $y_{MCMA}(k)$. For this issue, a lookup table of the $sinc$ function is constructed that consists of a matrix $\boldsymbol{H}$ of dimension $K \times (2.P+1)$ with a generic element:

$$h_{ij}(k) = sinc(\frac{i-1}{K} - j);\ 1 \le i \le K,\ -P \le j \le P, \quad (31)$$

where $K$ represents the inverse resolution over $T_s$ of the estimated delay $\hat{\tau}$. The elements of the $i$-th row of the matrix $\boldsymbol{H}$ are therefore identical to the samples of the truncated $sinc$ function with delay equal to:

$$\tau_i = (i-1)/K. \quad (32)$$

Thus, for a given $\tau_i$, equation (30) can be written as:

$$y_h(k) = \boldsymbol{h}_i^H \cdot \mathbf{u}(k), \tag{33}$$

where $\boldsymbol{h}_i$ is the $i$-th row of the matrix $\boldsymbol{H}$ and $\mathbf{u}(k)$ is given by:

$$\mathbf{u}(k) = [y_{MCMA}(k), \ldots, y_{MCMA}(k-(2P+1))]^T. \tag{34}$$

The estimated fractional time delay is obtained by using the gradient descent of the instantaneous squared error $|e_h|^2$ surface to locate the global minimum, i.e., using LMS [20]. This method is extended in this work to be applied to complex signals. The estimated gradient is equal to the derivative of $|e_h(k)|^2$ with respect to $\hat{\tau}$. The FTDE algorithm may be summarized as follows. The complex error signal $e_h(k)$ is given by:

$$\begin{aligned} e_h(k) &= y_{FD}(k) - y_h(k) \\ &= y_{FD}(k) - \sum_{i=-P}^{P} sinc(n-\hat{\tau}(k)).y_{MCMA}(k-n), \end{aligned} \tag{35}$$

where,

$$y_{FD}(k) = \mathbf{w}_{FD}^H \cdot \mathbf{x}_{e2\_D}(k), \tag{36}$$

$$\mathbf{x}_{e2\_D}(k) = \mathbf{x}_{e2}(k-(P+1)). \tag{37}$$

$\mathbf{x}_{e2}(k)$ is delayed by $(P+1)\cdot T_s$ to be aligned with the output of the filter $\boldsymbol{H}$ that has latency depending on its order value $M = 2P+1$ as shown in Fig.2b.
The estimated time delay can be adapted by minimizing the cost function given by:

$$J(\tau, \mathbf{w}_{FD}) = E[(e_h(k))^2] = E[(y_{FD}(k) - y_h(k))^2]. \tag{38}$$

The constrained LMS algorithm becomes:

$$\hat{\tau}(k+1) = \hat{\tau}(k) - \mu_4 \cdot \nabla J(\tau, \mathbf{w}_{FD}), \tag{39}$$

where $\tau_4$ is a small positive step size.

By differentiating the instantaneous error surface, $e_h(k)^2$, with respect to the estimated time delay, we have:

$$\begin{aligned} \frac{\partial(e_h(k)^2)}{\partial\hat{\tau}(k)} &= \frac{\partial e_h(k)}{\partial\hat{\tau}(k)}.e_h^*(k) + \frac{\partial e_h^*(k)}{\partial\hat{\tau}(k)}.e_h(k) \\ &= -\sum_{i=-P}^{+P} \frac{\partial(sinc(n-\hat{\tau}(k)))}{\partial\hat{\tau}(k)}.y_{MCMA}(k-n).e_h^*(k) \\ &\quad -\sum_{i=-P}^{+P} \frac{\partial(sinc(n-\hat{\tau}(k)))}{\partial\hat{\tau}(k)}.y_{MCMA}^*(k-n).e_h(k) \\ &= \sum_{i=-P}^{+P} f(n-\hat{\tau}(k)).y_{MCMA}(k-n).e_h^*(k) \\ &\quad + \sum_{i=-P}^{+P} f(n-\hat{\tau}(k)).y_{MCMA}^*(k-n).e_h(k), \end{aligned} \tag{40}$$

where

$$f(\upsilon) = \frac{\cos(\pi\upsilon) - sinc(\upsilon)}{\upsilon}. \tag{41}$$

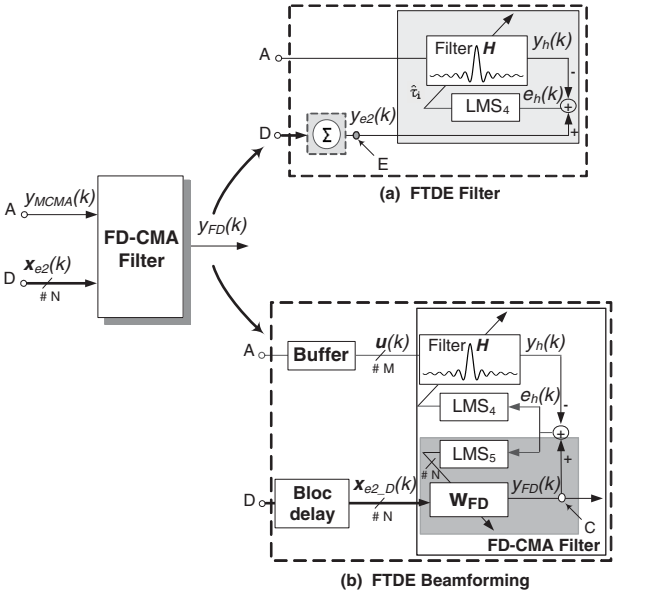


Fig. 2. (a) FTDE between signals received at points A and E seen as two spatially-separated antenna-array elements, (b) FD-CMA filter for fractional delay and path extraction.

Finally, the estimated time delay $\hat{\tau}$ is given by:

$$\begin{aligned} \hat{\tau}(k+1) =& \hat{\tau}(k) \\ &- \mu_4.[\sum_{n=-P}^{P} f(n-\hat{\tau}(k)).y_{MCMA}(k-n).e_h^*(k) \\ &+ \sum_{n=-P}^{P} f(n-\hat{\tau}(k)).y_{MCMA}^*(k-n).e_h(k)]. \end{aligned} \tag{42}$$

In our simulations, lookup tables of $cos$ and $sinc$ functions are constructed for different values of $\upsilon$ and used to calculate $f(n-\hat{\tau}(k))$. At each iteration, the integer part of $(\hat{\tau}(k)\cdot K+1)$ is used to locate the $i$-th row of the matrix $\boldsymbol{H}$, i.e. $\boldsymbol{h}_i$ that is used to delay the signal $y_{MCMA}(k)$ using (33) (see the Appendix).

*2) Beamforming for fractional delay path extraction:* Now to extract the fractional delay path, the weight vector of the FD-CMA filter is adapted using LMS by minimizing the cost function given in (38) as follows:

$$\mathbf{w}_{FD}(k+1) = \mathbf{w}_{FD}(k) + \mu_5 \cdot e_h^*(k) \cdot \mathbf{x}_{e2\_D}(k), \tag{43}$$

where $\mu_5$ is a small step size.

### *F. Coherent MRC with hard Decision Feedback Identification*

The paths $y_{MCMA}$, $y_{FD}$ and $y_{ID}$, estimated by the filters MCMA, FD-CMA and ID-CMA, respectively, possess a common phase ambiguity, since they are sequentially extracted using $y_{MCMA}$ as a reference signal. As a result, a combination based on a simple addition of the estimated paths can only be constructive and it represents the output of a coherent Equal Gain Combiner (EGC). After appropriate delay alignments, the final estimated signal is given by EGC combining of the extracted paths (cf. EGC block in Fig. 3) as follows:

$$y(k) = y_{MCMA}(k) + y_{FD}(k) + y_{ID}(k+1). \tag{44}$$

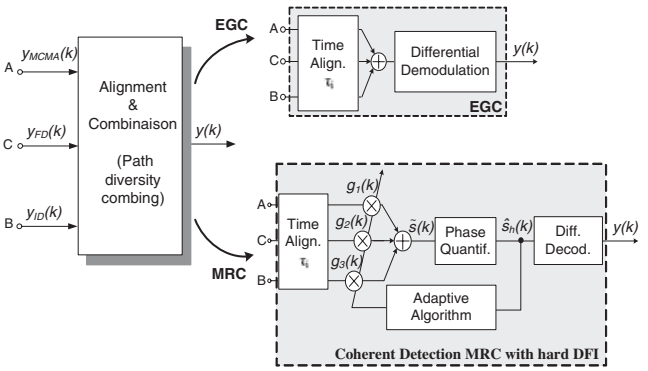


Fig. 3. Path diversity combining stage for the SBB using EGC or Coherent MRC with hard DFI.

For a Differential Binary Phase Shift Keying (DBPSK) modulation scheme, where the common phase ambiguity is actually a sign ambiguity, an EGC is equivalent to MRC. However, for higher order modulations such as Differential Quadrature Phase Shift Keying (DQPSK), where the common phase ambiguity is an unknown angular rotation, more substantial improvement compared to EGC can be obtained by implementing coherent MRC with hard DFI as shown in MRC block in Fig. 3, which strives to force this common phase ambiguity to known quantized values that keep the constellation invariant by rotation [26], thereby allowing coherent demodulation and MRC detection. In the first step, all the paths $y_{MCMA}(k)$, $y_{FD}(k)$ and $y_{ID}(k)$ are aligned by appropriate additional delays, and then scaled by an MRC weighting vector $\boldsymbol{g}(k)$. The summation of these scaled paths, $\tilde{s}(k)$, is given by:

$$\tilde{s}(k) = \boldsymbol{g}^H(k) \cdot \boldsymbol{y}_d(k), \tag{45}$$

where,

$$\boldsymbol{y}_d(k) = [y_{MCMA}(k)\ y_{FD}(k)\ y_{ID}(k+1)]^T, \tag{46}$$

$$\boldsymbol{g}(k) = [g_1(k)\ g_2(k)\ g_3(k)]^T. \tag{47}$$

In the next step, $\tilde{s}(k)$ is quantized by making a hard decision to match it to a tentative symbol $\hat{s}_h(k)$. This coherent-detection operation can be expressed as follows:

$$\hat{s}_h(k) = Hard\{\tilde{s}(k)\} = arg_{a_k \in A_M}\ min\{|\tilde{s}(k) - a_k|\}, \tag{48}$$

where $A_M$ represents the MPSK modulation constellation defined by:

$$\begin{aligned} A_M &= \{\ldots, a_k, \ldots\} \\ &= \{\ldots, e^{\frac{j((2k-1)-\delta(M-2))\pi}{M}}, \ldots\};\ k \in \{1, \ldots, M\}. \end{aligned} \tag{49}$$

Since $\hat{s}_h(k)$ provides a selected estimate of the desired signal, it can be used as a feedback reference signal to update the weight vector $\boldsymbol{g}(k)$ using LMS-type adaptation referred to as Decision Feedback Identification (DFI):

$$\mathbf{g}(k+1) = \mathbf{g}(k) + \mu_6 \cdot (\mathbf{y}_d(k) - \mathbf{g}(k) \cdot \hat{s}_h(k)) \cdot \hat{s}_h^*(k), \tag{50}$$

where $\mu_6$ is an adaptation step-size.

It is this DFI procedure that enables coherent MRC detection by forcing the common phase ambiguity of the extracted paths to a value by which the constellation is invariant by rotation [26]. Finally the desired output signal $y(k)$ is estimated from $\hat{s}_h(k)$ by differential decoding, as shown in Fig.3, instead of differential demodulation needed previously with simple EGC. This final decoding step is expressed by:

$$y(k) = \hat{s}_h(k) \cdot \hat{s}_h^*(k-1). \tag{51}$$

The proposed technique enabling MRC path diversity combining offers an $SNR$ gain of about 2 $dB$ gain compared to simple EGC implementation [25, 26].

TABLE I
SIMULATION PARAMETERS

| | |
|---|---|
| Modulation | Modulation DBPSK or DQPSK |
| Antenna array type | Linear uniform, with $\lambda/2$ element spacing |
| Antenna array size | 2 elements or 4 elements |
| Max. Doppler frequency | $f_{d1} = 20\ Hz$ and $f_{d2} = 35\ Hz$ |
| Channel model | Type-A: Rayleigh fading with $f_{d1}$<br>Type-B: Rayleigh fading with $f_{d2}$ |
| Adaptive algorithm | CMA & LMS |
| Carrier Frequency | $f_c = 2.4\ GHz$ |
| Noise | AWGN |
| Filter order | $M = 21$ |
| Path resolution | $K = 200$, i.e. $T_r = 0.005\ T_s$ |
| Step sizes | $\mu = 0.009;\ \mu_1 = 0.008;\ \mu_2 = 0.0095;$<br>$\mu_3 = 0.008;\ \mu_4 = 0.001;\ \mu_5 = 0.009$<br>and $\mu_6 = 0.001$. |
| Number of symbol | 10.000 |

## IV. Computer Simulation Results

In this section, simulation results are presented to assess the performance of the proposed SBB method and to compare it with MCMA beamforming [22]. A two-element array with half-wavelength spacing is considered. A desired signal is propagated along four multipaths to the antenna array while the interference and noise are simulated as additive white Gaussian noise. The first path is direct with a path arrival-time delay $\tau_1 = 0$. The second and third paths arrive, respectively, with delays $\tau_2$ and $\tau_3$ lower than the sampling interval, and the last path arrives with delay $\tau_4 = T_s$. Differential encoding is employed to overcome the phase ambiguity in the signal estimation. Performance study was carried out with two channel models and for two kinds of modulation (DBPSK and DQPSK). Type-A channel is Rayleigh fading with a Doppler shift $f_{d1} = 20\ Hz$. Type-B channel is Rayleigh fading with a higher Doppler shift $f_{d2} = 35\ Hz$. The use of these two Doppler frequencies reflects the typical range of the vehicle speed in underground environments[3]. The Bit Error Rate ($BER$) performance for different Doppler frequencies ($f_{d1}$ and $f_{d2}$) was also studied. The figure of merit is the required $SNR$ to achieve a $BER$[4] below 0.001. Table 1 summarizes the system parameters for the computer simulations.

Figures 4 and 5 show the measured $BER$ performance versus $SNR$ of SBB and MCMA for Type-A and -B channels, with different values of $\tau_2$ and $\tau_3$ using a DBPSK modulated signal. As expected, it can be noted that for both algorithms,

[3]For operations at a carrier frequency $f_c = 2.4\ GHz$ and vehicle speeds $v_1 = 10km/h$, and $v_2 = 15km/h$, we found approximately that $f_{d1} = 20\ Hz$ and $f_{d2} = 35Hz$.

[4]The $BER$ is calculated after steady-state convergence to avoid biasing the results.

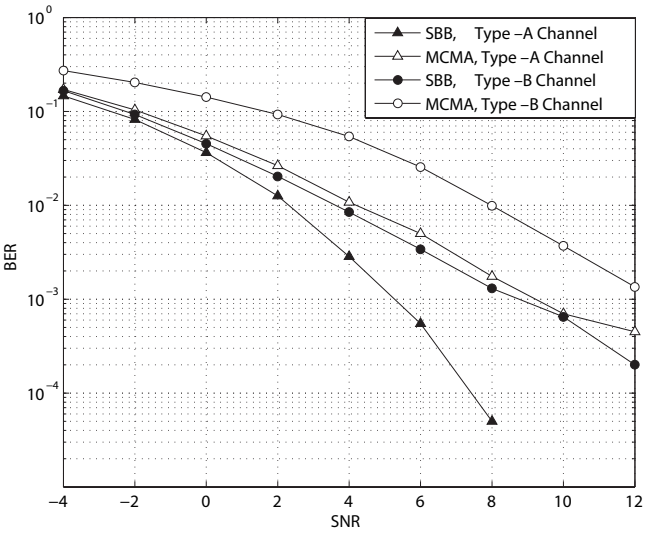


Fig. 4. $BER$ performance versus $SNR$ with $\tau_2 = 0.4\ T_s$ and $\tau_3 = 0.8\ T_s$ for DBPSK modulation scheme using 2-antenna elements array.

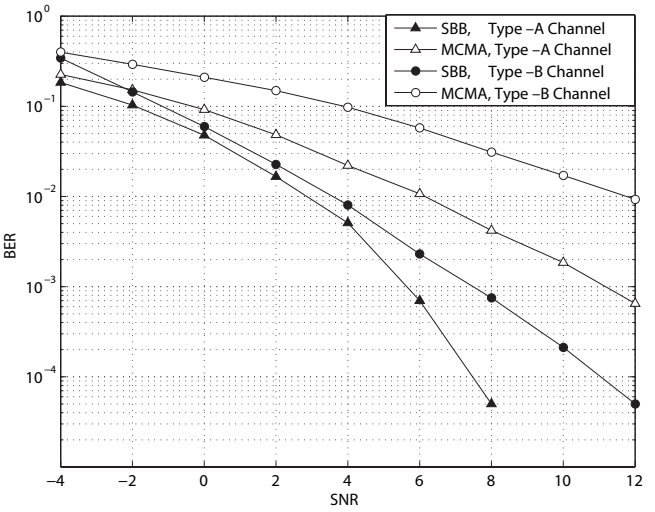


Fig. 5. BER performance versus SNR with $\tau_2 = 0.3\ T_s$ and $\tau_3 = 0.7\ T_s$ for DBPSK modulation scheme using 2-antenna elements array.

the $BER$ performance decreases with increasing Doppler frequency values. Despite the speed increasing due to the Doppler effect, the proposed algorithm SSB provides significant gains and outperforms MCMA by approximately $5\ dB$ for both channel environments (A and B).

Let us now study the convergence rate of the proposed SBB method compared to the MCMA algorithm for the Type-A channel with $\tau_2 = 0.4\ T_s$ and $\tau_3 = 0.8\ T_s$ at $2.4\ GHz$ and for $SNR = 4\ dB$. Figure 6 illustrates the average $BER$ in terms of the number of iterations for the first $8000$ samples. A benchmark comparison with AAA using the LMS algorithm is also provided. From Fig. 6, it can be seen that the LMS algorithm is the fastest one followed by the MCMA and than the SBB algorithms. However, the proposed SBB algorithm reaches a much lower steady-state $BER$ after convergence within a shorter delay compared to AAA and MCMA.

Here we discuss a trade-off between the hardware complexity related to the delay resolution implementation and the

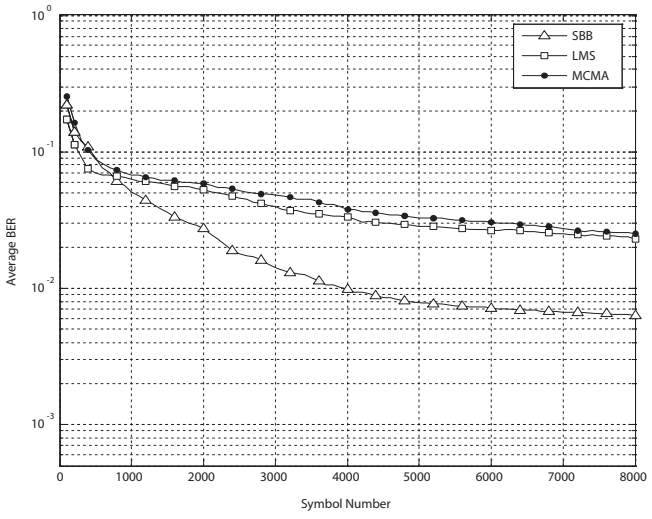


Fig. 6. The real-time performance of the proposed system compared with the MCMA and LMS algorithms at $SNR = 4\ dB$ for DBPSK modulation scheme using 2-antenna elements array.

$BER$ performance. As mentioned above, $K$, given in equation (32), represents the number of the tap filter coefficients used to implement the fractional delay resolution. For instance, when $K = 10$, the delay resolution is equal to $T_r = 1/(K.T_s) = 0.1\ T_s$. By increasing the value of $K$, we increase the FTDE resolution and consequently the FTDE filter will be able to estimate faithfully the fractional delay path which will in turn improve the $BER$ performance. On the other hand, increasing $K$ increases the hardware complexity needed to implement the FTDE. To find an optimal trade-off between resolution and hardware complexity, several simulations with different values of $K$ in terms of $BER$ performance were conducted.

Figure 7 illustrates the simulated $BER$ performance versus $SNR$ of the SBB for Type-A channel environment at different values of $T_r$. From this figure, it can be seen that the resolution of $K$ impacts greatly the $BER$ performance when $K$ is less than $50$. For $K$ greater than $50$, the optimal performance is attained and further increase of the $K$ value is unnecessary.

For high order modulation using DQPSK, Figures 8 and 9 illustrate the $BER$ performance versus $SNR$ for SBB using MRC or EGC in the combining step for Type-A and -B channels with $\tau_2 = 0.4\ T_s$ and $\tau_3 = 0.8\ T_s$, respectively, at $2.4\ GHz$. A benchmark comparison with AAA using MCMA is also provided. For the type-A channel, the results show that SBB with MRC provides a good enhancement and outperforms SBB with EGC and the AAA using MCMA by approximately $2\ dB$ and up to $7\ dB$ at a required $BER = 0.001$, respectively (Fig. 8). For the type- B channel with higher Doppler frequency, the measured results show that SBB with MRC maintains its advantage compared to SBB with EGC and to the AAA using MCMA where improvements of approximately $2\ dB$ and up to $7\ dB$ at a required $BER = 0.001$ are obtained, respectively (Fig. 9).

Figure 10 shows the measured $BER$ performance versus $SNR$ for SBB using MRC or EGC in the combining step and with MCMA-AAA for Type-A channel using four antenna elements ($N = 4$). Again, it is clear that the SBB using

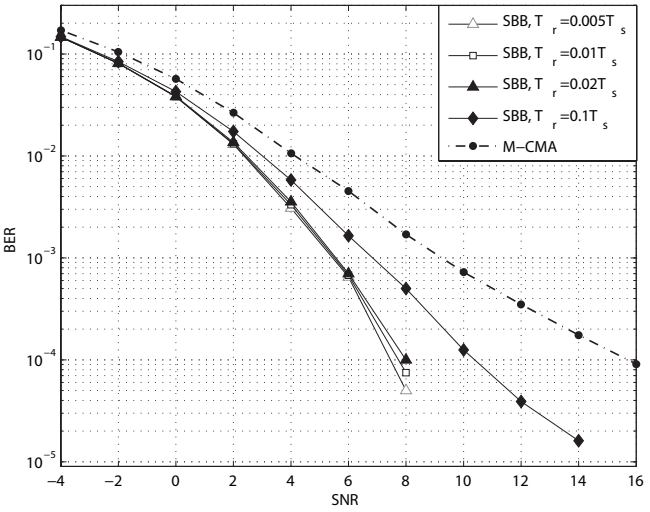


Fig. 7. $BER$ performance versus $SNR$ in Type -A Channel for $\tau_2 = 0.4\,T_s$ and $\tau_3 = 0.8\,T_s$ when $T_r$ is varied using 2-antenna elements array.

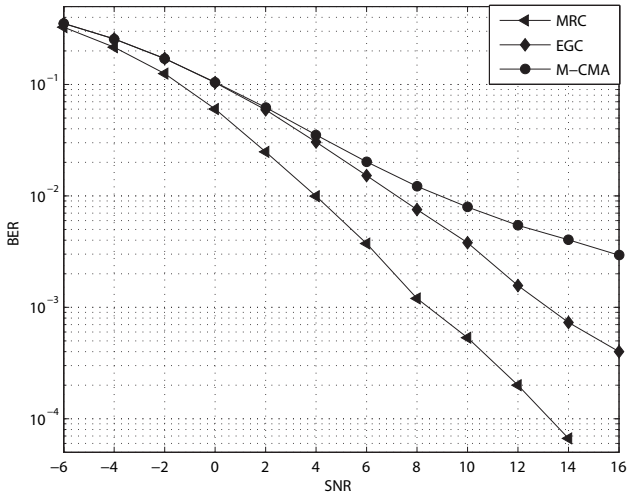


Fig. 8. $BER$ performance versus $SNR$ for Type -A Channel with $\tau_2 = 0.4\,T_s$ and $\tau_3 = 0.8\,T_s$ for DQPSK modulation scheme using 2-antenna elements array.

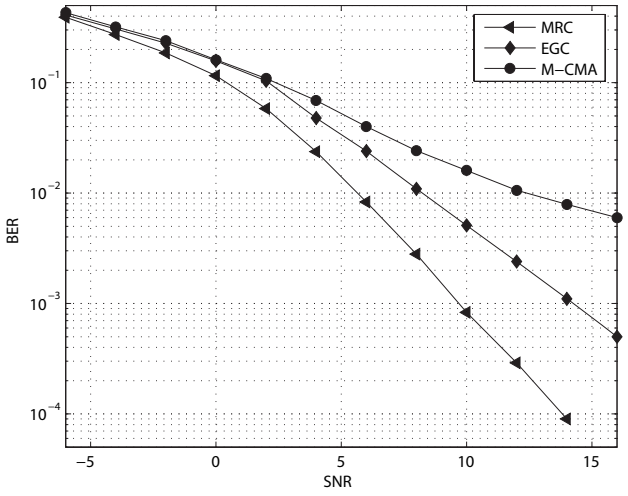


Fig. 9. $BER$ performance versus SNR for Type -B Channel with $\tau_2 = 0.4\,Ts$ and $\tau_3 = 0.8\,Ts$ for DQPSK modulation scheme using 2-antenna elements array.

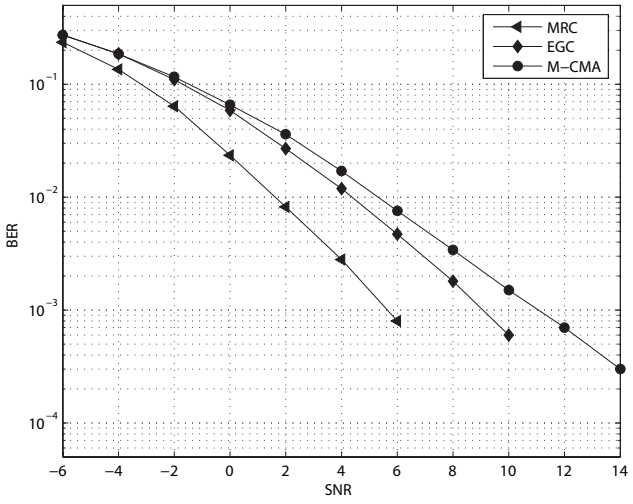


Fig. 10. $BER$ performance versus $SNR$ for Type -A Channel with $\tau_2 = 0.2\,T_s$ and $\tau_3 = 0.8\,T_s$ for DQPSK modulation scheme using 4-antenna elements array.

the proposed MRC is more efficient than both previous SBB versions using EGC and conventional MCMA algorithm.

## V. Conclusion

In this paper, a new approach using sequential blind spatial-domain path-diversity beamforming (SBB) to remedy the ISI and isi problems has been proposed. Using jointly CMA, LMS and adaptive FTDE filtering, this approach has been designed to sequentially recover multipath rays to maximize the received power by extracting all dominant multipaths. MCMA is used to estimate the strongest path while the integer path delay is estimated sequentially using adapted LMS with the first beamformer output as a reference signal. A new synchronization approach for multipath propagation, based on combining a CMA-AAA and adaptive fractional time delay estimation filtering, has been proposed to estimate the fractional path delay. It should be noted that this proposed SBB architecture can be generalized for an arbitrary number of received paths causing ISI where several concurrent filters (ID-CMA and FD-CMA) can be implemented to resolve the different paths. Finally, to combine these extracted paths, an enabling MRC path diversity combiner with hard DFI has also been proposed. Simulation results show the effectiveness of the proposed SBB receiver especially at high $SNR$, where it is expected to operate in a typical underground wireless environment [1].

## Appendix I

Fractional-Delay filters are a type of digital filter designed for band-limited interpolation. If a limited-band signal $x(t)$ is delayed by $D$, the signal $y(t) = x(t - D)$ is obtained. By sampling this signal at time instances $t = k \cdot T$, where $T$ is the sampling interval which is assumed without loss of generality to be unity, the delayed version of the discrete-time signal $x(k)$ may be represented as [20]:

$$y(k) = x(k - D) = \sum_{i=-\infty}^{+\infty} h_{id}(n).x(k - n), \qquad (52)$$

where $D$ is a positive real number that can be split into integer and fractional parts as:

$$D = int(D) + \tau. \tag{53}$$

The impulse response in Equation (52) is an ideal impulse response and so called an ideal fractional-delay filter whose coefficients are given by [20]:

$$h_{id}(n) = sinc(n - D), \tag{54}$$

for $n \in \mathbb{Z}$ and $D \in \mathbb{R}$.

If $D$ is a fractional number, i.e. $0 < \tau < 1$, the impulse response has non-zero values for all $n$:

$$0 < \tau < 1 \quad \rightarrow h_{id}(n) \neq 0, \quad \forall\ n \in \mathbb{Z}. \tag{55}$$

Figure 11 shows the ideal impulse response when $D = 3.0$ and $D = 3.4$ samples. We notice that when the delay $D$ is an integer, only one sample is non-zero because the zero crossings of the $sinc$ function coincide with the other sampling points. However, when the delay $D$ is a fractional number, all the samples (black circles) on the interval $(-\infty, +\infty)$ are non-zero. For this reason, the impulse response corresponds to an infinite-length noncausal filter which cannot be made causal by a finite shift in time. In addition, the filter is not stable since the impulse response is not absolutely summable. The ideal fractional delay filter is thus nonrealizable. To produce a realizable fractional delay filter, some finite-length, causal approximation for the $sinc$ function has to be used.

For the time delay estimation process, only the estimated time delay $\hat{\tau}_i(k)$ is adapted in this work, and it is used as an index to obtain the vector $\boldsymbol{h}_i$ from a lookup table. As mentioned previously, this lookup table is a two-dimensional matrix called $\boldsymbol{H}$ of size $K \times (2P+1)$ that contains samples of the $sinc$ function with delay ranging from 0 to $(K-1)/K$. For a given vector $\tau$ with theoretically delayed value elements, $\tau_i$ is given by (32) and repeated here for convenience:

$$\tau_{i(theor)} = \frac{i-1}{K}, \quad 1 \leq i \leq K. \tag{56}$$

Then,

$$i = \tau_{i(theor)} \cdot K + 1. \tag{57}$$

So, at each iteration, the integer part of $(\hat{\tau}_i(k) \cdot K + 1)$ is used to locate the $i$-th row of the matrix $\boldsymbol{H}$, i.e. $\boldsymbol{h}_i$ that is used to delay the signal $y_{MCMA}(k)$ using (33).

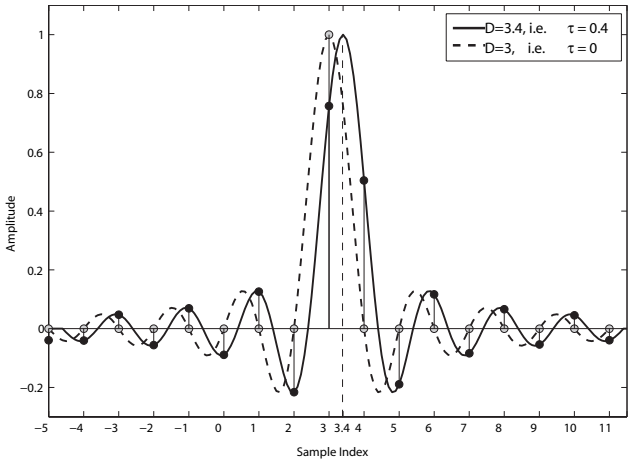


Fig. 11. Ideal $sinc$ impulse response shifted by $D$ and sampled at sampling interval.

## REFERENCES


[1] C. Nerguizian, C. Despins, S. Affes, and M. Djadel, "Radio-channel characterization of an underground mine at 2.4 $GHz$ wireless communications," *IEEE Trans. Wireless Commun.*, vol. 4, no. 5, pp. 2441-2453, Sept. 2005.

[2] R. Y. Chao and K. S. Chung, "A low profile antenna array for underground mine communication," in *Proc. ICCS 1994*, vol. 2, pp. 705-709.

[3] S. R. Saunders, *Antenna and Propagation for Wireless Communication Systems.* Chichester, England: John Wiley & Sons, Ltd., 1999.

[4] H. Amca, T. Yenal, and K. Hacioglu, "Adaptive equalization of frequency selective multipath fading channels based on sample selection," *Proc. IEE on Commun.*, vol. 146, no. 1, pp. 55-60, Feb. 1999.

[5] Y. Sanada, and Q. Wang, "A co-channel interference cancellation technique using orthogonal convolutional codes on multipath Rayleigh fading channel," *IEEE Trans. Veh. Technol.*, vol. 46, no. 1, pp. 114-128, Feb. 1997.

[6] C. Cozzo and B. L. Hughes, "Space diversity in presence of discrete multipath fading channel," *IEEE Trans. Commun.*, vol. 51, no. 10, pp. 1629-1632, Oct. 2003.

[7] T. Tanaka, "A study on multipath propagation characteristics for RAKE receiving technique," in *Proc. 5th IEEE International Symposium on Personal, Indoor and Mobile Radio Commun.*, Sept. 1994, vol. 2, pp. 711-714.

[8] J. H. Stott, "The how and why of COFDM," tutorial COFDM, BBC Research and Development, http://www.ebu.ch/en/technical/trev/trev_278-stott.pdf.

[9] D. McNeil, A. T. Denidni, and G. Y. Delisle, "Output power maximization algorithm performance of dual-antenna for personal communication handset applications," in *Proc. IEEE Antennas and Propagation Society International Symposium*, July 2001, vol. 1, pp. 128-131.

[10] S. Bellofiore, C. A. Balanis, J. Foutz, and A. S. Spanias, "Smart-antenna systems for mobile communication networks, part 1: overview and antenna design," *IEEE Antennas Propag. Mag.*, vol. 44, no. 3, pp. 145-154, June 2002.

[11] S. Bellofiore, J. Foutz, C. A. Balanis, and A. S. Spanias, "Smart-antenna systems for mobile communication networks, part 2: beamforming and network throughput," *IEEE Antennas Propag. Mag.*, vol. 44, no. 4, pp. 106-114, Aug. 2002.

[12] W. C. Lee and S. Choi, "Adaptive beamforming algorithm based on eigen-space method for smart antennas," *IEEE Commun. Lett.*, vol. 9, no. 10, pp. 888-890, Oct. 2005.

[13] W. S. Youna and C. K. Un, "Robust adaptive beamforming based on the eigen-structure method," *IEEE Trans. Signal Processing*, vol. 42, no. 6, pp. 1543-1547, June 1994.

[14] L. C. Godara, "Applications of antenna arrays to mobile communications, part I: performance improvement, feasibility, and system considerations," *Proc. IEEE*, July 1997, vol. 85, no. 7, pp. 1031-1060.

[15] B. Widrow, P. E. Mantey, L. J. Griffiths, and B. B. Goode, "Adaptive antenna systems," *Proc. IEEE*, vol. 55, no. 12, pp. 2143-2159, Dec. 1967.

[16] Y. Tanabe, *et al.*, "An adaptive antenna for spatial-domain path-diversity using a super-resolution technique," in *Proc. IEEE VTC'00*, May 2000, vol. 1, pp. 1-5.

[17] Y. Ogawa, K. Fujishima, and T. Ohgane, "Weighting factors in spatial-domain path-diversity using an adaptive antenna," in *Proc. IEEE VTC'99*, May 1999, vol. 3, pp. 2184-2188.

[18] S. Affes and P. Mermelstein, "A new receiver structure for asynchronous CDMA: STAR-the spatio-temporal array-receiver," *IEEE J. Select. Areas Commun*, vol. 16, no. 8, pp. 1411-1422, Oct. 1998.

[19] D. T. M. Slock, "Blind joint equalization of multiple synchronous mobile users using over sampling and/or multiple antennas," in *Proc. IEEE Asilomar Conference on Signals, Systems and Computers*, 1994, vol. 2, pp. 1154-1158.

[20] H. C. So, P. C. Ching, and Y. T. Chan, " New algorithm for explicit adaptation of time delay," *IEEE Trans. Signal Processing*, vol. 42, no. 7, pp. 1816-1820, July 1994.

[21] V. Valimaki and T. I. Laakso, "Principles of fractional delay filters," in *Proc. IEEE ICASS*, June 2000, vol. 6, pp. 3870-3873.

[22] K. N. Oh and Y. O. Chin, "New blind equalization techniques based on constant modulus algorithm," in *Proc. Global Telecommunications Conference*, Nov. 1995, vol. 2, pp. 865-869.

[23] S. A. Fares, T. A. Denidni, and S. Affes, "Sequential blind beamforming algorithm using combined CMA/LMS for wireless underground communications," in *Proc. IEEE VTC'04*, Sept. 2004, vol. 5, pp. 3600-3604.
[24] S. A. Fares, T. A. Denidni, S. Affes, and C. Despins, "CMA/fractional-delay sequential blind beamforming for wireless multipath communications," in *Proc. IEEE VTC'06*, May 2006, vol. 6, pp. 2793-2797.
[25] S. A. Fares, T. A. Denidni, S. Affes, and C. Despins, "Efficient sequential blind beamforming for wireless underground communications," in *Proc. IEEE VTC'06*, Sept. 2006, pp. 1-4.
[26] S. Affes and P. Mermelstein, "Adaptive space-time processing for wireless CDMA," chapter 10, pp. 283-321, in *Adaptive Signal Processing: Application to Real-World Problems*, J. Benesty and A. H. Huang, eds. Berlin: Springer, 2003.
[27] M. Boutin, S. Affes, C. Despins, and T. A. Denidni, "Statistical modelling of a radio propagation channel in an underground mine at 2.4 and 5.8 GHz," in *Proc. IEEE VTC'05*, June 2005, vol. 1, pp. 78-81.
[28] H. Furukawa, Y. Kamio, and H. Sasaoka, "Cochannel interference reduction and path-diversity reception technique using CMA adaptive array antenna in digital land mobile communications," *IEEE Trans. Veh. Technol.*, vol. 50, no. 2, pp. 605-616, March 2001.

**Salma A. Farès** received the B.S degree from Mohammed V University, Rabat, Morocco, in 1999, and M.Sc and Ph.D. degrees, respectively, in electrical engineering from University of Québec in Trois Rivières, in 2003, and in telecommunication from INRS-ÉMT, University of Québec, Montréal, Qc, Canada, in 2007. She is currently postdoctoral fellow with Wireless Signal Processing & Networking Laboratory, Tohoku University, Sendai, Japan. Her research interests include adaptive antenna arrays, virtual cellular network, sensor networks, and signal processing for telecommunication applications.

**Tayeb A. Denidni** (M'98-SM'04) received the B.Sc. degree in electronic engineering from the University of Setif, Setif, Algeria, in 1986, and the M. Sc. and Ph.D. degrees in electrical engineering from Laval University, Quebec City, QC, Canada, in 1990 and 1994, respectively. From 1994 to 1996, he was an Assistant Professor with the engineering department, Université du Quebec à Rimouski (UQAR), Rimouski, QC, Canada. From 1996 to 2000, he was also an Associate Professor at UQAR, where he founded the Telecommunications laboratory. Since August 2000, he has been with the Personal Communications Staff, Institut National de la Recherche Scientifique (INRS-EMT), Université du Québec, Montréal, QC, Canada. He founded the RF Laboratory, INRS-ÉMT, for graduate student research in the design, fabrication, and measurement of antennas.

He possesses ten years of experience with antennas and microwave systems and is leading a large research group consisting of two research scientists, five Ph.D. students, and three M.S. students. Over the past ten years, he has graduated numerous graduate students. He has served as the Principal Investigator on numerous research projects on antennas for wireless communications. His current research interests include planar microstrip filters, dielectric-resonator antennas, electromagnetic-bandgap (EBG) antennas, antenna arrays, and microwave and RF design for wireless applications. He has authored over 50 papers in refereed journals. He has also authored or coauthored over 80 papers and invited presentations in numerous national and international conferences and symposia. Since 2006, he has also served as an associate editor for *IEEE Antennas and wireless Propagation Letters*. Dr. Denidni is a member of the Order of Engineers of the Province of Quebec, Canada. He is also a member of URSI (Commission C).

**Sofiène Affès** (M'94, SM'04) received the Diplôme d'Ingénieur in electrical engineering in 1992, and the Ph.D. degree with honors in signal processing in 1995, both from the École Nationale Supérieure des Télécommunications (ENST), Paris, France.

He has been since with INRS-ÉMT, University of Quebec, Montreal, Canada, as a Research Associate from 1995 till 1997, then as an Assistant Professor till 2000. Currently he is an Associate Professor in the Personal Communications Group. His research interests are in wireless communications, statistical signal and array processing, adaptive space-time processing and MIMO. From 1998 to 2002 he has been leading the radio-design and signal processing activities of the Bell/Nortel/NSERC Industrial Research Chair in Personal Communications at INRS-ÉMT, Montreal, Canada. Currently he is actively involved in a major project in wireless of PROMPT-Québec (Partnerships for Research on Microelectronics, Photonics and Telecommunications).

Professor Affes is the co-recipient of the 2002 Prize for Research Excellence of INRS and currently holds a Canada Research Chair in High-Speed Wireless Communications. He served as a General Co-Chair of the IEEE VTC'2006-Fall conference, Montréal, Canada, and currently acts as a member of the Editorial Board of the *Wiley Journal on Wireless Communications & Mobile Computing* and of the *IEEE Transactions on Wireless Communications*.

**Charles L. Despins** (S'93-M'94-SM'02) received a Bachelor's. degree in electrical engineering from McGill University, Montréal, QC, Canada, in 1984, and Master's. and Ph.D. degrees from Carleton University, Ottawa, ON, Canada, in 1987 and 1991, respectively. He was, from 1992 to 1996, a Faculty Member of the Institut National de la Recherche Scientifique (INRS), Université du Québec, Montréal, Canada, following employment in 1984-85 with CAE Electronics as a Member of the Technical Staff, and in 1991-92 with the Department of Electrical and Computer Engineering, École Polytechnique de Montréal, Canada, as a Lecturer and a Research Engineer. From 1996 to 1998, he was with Microcell Telecommunications Inc., a Canadian GSM operator, and was responsible for industry standard and operator working groups, as well as for technology trials and technical support for GSM joint venture deployments in China and India. From 1998 to 2003, he was Vice-President & Chief Technology Officer of Bell Nordiq Group Inc., a wireless & wireline network operator in northern and rural areas of Canada. Since 2003, he has been president and CEO of PROMPT-Quebec, a university-industry research consortium in the field of information and communications technologies. He remains an Adjunct Professor at INRS-EMT, Montréal, QC, Canada with research interests in wireless communications.

Dr. Despins was awarded the IEEE Vehicular Technology Society Best Paper of the Year prize in 1993 as well as the Outstanding Engineer Award in 2006 from IEEE Canada. He is a Member of the Order of Engineers of Québec and is also a Fellow of the Engineering Institute of Canada.